Microgravity Science and Technology (2022) 34: 47
https://doi.org/10.1007/s12217-022-09968-x

ORIGINAL ARTICLE

Enhanced Boiling Heat Transfer Performance on Mini-pin-finned Copper Surfaces in FC-72

Hongqiang Chen[1] · Pengzhuo Xu[2] · Wangfang Du[3,4] · Yonghai Zhang[1] · Zhiqiang Zhu[3,4] · Jinjia Wei[1,5]

Received: 21 March 2022 / Accepted: 19 May 2022 / Published online: 6 June 2022
© The Author(s), under exclusive licence to Springer Nature B.V. 2022

Abstract
The uniformly distributed mini-pin-fins on the copper surface were designed and processed, and the enhanced boiling heat transfer performance on mini-pin-finned copper surfaces in FC-72 was investigated. The smooth copper surface was used as the experimental comparison group. The effect of the copper fin height, spacing, and width on the pool boiling heat transfer performance and the fin efficiency were investigated. At the same liquid subcooling, the critical heat flux and heat transfer coefficient of the uniformly distributed mini-pin-finned copper surface increased with the copper fin height, decreased with the rise of the copper fin spacing and fin width. The fin efficiency increases with the rise of the fin height, spacing, and width. The critical heat flux of the mini-pin-finned copper surface (PF0.3–0.2–2) reached 115.4 W·cm^{-2} at liquid subcooling of 25 K and increased by about 3.62 times compared with the smooth copper surface, and the heat transfer efficiency of mini-pin-finned copper surface (PF0.5–0.2–2) exceeded 95%.

Keywords Pool boiling · Heat transfer enhancement · Mini-pin-fins · Critical heat flux

Introduction

With the development of The Times and society, human beings are more and more closely connected with various electronic devices. At the same time, the degree of integration of high-performance electronic devices is also rapidly improving, and the heat flux of high-power and high-performance electronic devices also reaches 1000 W·cm^2 (Lee and Mudawar 2008). Lack of effective heat dissipation will cause chip performance degradation or damage, so effective heat dissipation methods and theories have become a vital reason to restrict the further development of high-performance electronic equipment. It has become urgent work to study electronic devices efficient heat dissipation technology (He et al. 2021; Wei et al. 2009; Bar-Cohen and Wang 2009).

The traditional air-cooling and water-cooling cooling methods have been widely used due to the advantages of simple structure and mature technology. Still, their relatively low heat transfer coefficient has been challenging to meet the new generation of high-performance equipment requirements for high heat flux heat dissipation. Unlike Single-phase liquid cooling schemes rely entirely on heat removal by raising the coolant's sensible heat, two-phase schemes capitalize on both sensible and latent heat of the coolant. Thereby, two-phase schemes allow for more heat

This article belongs to the Topical Collection: Research Pioneer and Leader of Microgravity Science in China: Dedicated to the 85th Birthday of Academician Wen-Rui Hu
Guest Editors: Jian-Fu Zhao, Kai Li

✉ Yonghai Zhang
zyh002@mail.xjtu.edu.cn

✉ Zhiqiang Zhu
zhuzhiqiang@imech.ac.cn

[1] School of Chemical Engineering and Technology, Xi'an Jiaotong University, Xi'an, Shaanxi 710049, People's Republic of China

[2] Xi'an Navigation Technology Research Institute, Xi'an, Shannxi 710068, People's Republic of China

[3] Key Laboratory of Microgravity, Institute of Mechanics, Chinese Academy of Sciences, Beijing 100190, People's Republic of China

[4] School of Engineering Science, University of Chinese Academy of Sciences, Beijing 100049, People's Republic of China

[5] Key Laboratory of Multiphase Flow in Power Engineering, Xi'an Jiaotong University, Xi'an 710049, People's Republic of China

evacuation while retaining relatively low device temperature (Liang and Mudawar 2021). Boiling heat transfer (Xu et al. 2021; Wang et al. 2021) is a way to solve the heat dissipation of electronic devices under high heat fluxes by using latent heat of the phase transformation process, common boiling heat transfer methods include pool boiling (Kim et al. 2018; Dhadda et al. 2021; Godinez et al. 2021; Moghadasi and Saffari 2021), flow boiling (Song et al. 2019; Gupta and Misra 2021), jet impingement (Devahdhanush and Mudawar 2021; Adeoye et al. 2021) and so on. Pool boiling is also the simplest, economic and reliable scheme of all phase change heat transfer, and application scenarios often involve normal gravity (Kim et al. 2018; Dhadda et al. 2021; Godinez et al. 2021) and microgravity environment (Zhao et al. 2009; Li et al. 2022).

In recent years, researchers have strengthened the heat transfer capacity of pool boiling by various methods, and these methods include machining cylindrical structures (Nguyen et al. 2018; Pastuszko 2012), increasing surface roughness (Dadjoo et al. 2017; Kim 2014), changing surface wettability (Kim et al. 2014; Li et al. 2018), and rising micro-nano structures (Jothi Prakash and Prasanth 2018; Patil and Kandlikar 2014; Ray et al. 2016) and so on. The most effective way to improve the heat transfer capacity of the surface is to increase the heat transfer area, which can increase the number of nucleation sites on the surface. The rough surface (Tran et al. 2020) is mainly made by mechanical processing (Fan et al. 2020), the chemical method (Jung and Kwak 2006), and so on. The purpose is to improve the surface roughness and increase the surface heat transfer area. In addition, the rough surface has more nucleation sites, smaller bubble departure radius, and higher bubble departure frequency, which are the reasons for increasing the boiling heat transfer coefficient. The sintered surface (Byon et al. 2013) is the porous surface obtained by sintering after the powder is formed, and its large porosity can enhance the heat transfer (Li et al. 2011; Thiagarajan et al. 2015), and if nanostructures were added to the sintered porous surface (Li et al. 2020), the increase of nucleation sites on the surface would significantly enhance Heat Transfer Coefficient (HTC). The etched surface (Kim et al. 2015) made by etching the surface area using chemical reagents could effectively increase the heat transfer area. FC-72 was used as the working medium for enhanced boiling heat transfer research for many years in our group, many silicon-based modified surfaces have been developed, including bi-structured surfaces (Kong et al. 2018), inhomogeneous wetting surface (Yu et al. 2020), nonuniform micro-pillars surface (Duan et al. 2020), micro-nano composite structure surface (Zhou et al. 2019), the heat flux can be realized within the scope of 50–200 $W.cm^{-2}$. The micro-nano structures grown on the surface of carbon nanotubes (Bertossi et al. 2015) can provide a large number of nucleation sites, and can reduce the bubble departure radius, produce a large number of stable small bubbles, and improve the heat transfer capacity of the surface. Micro-machined surface by using milling cutter (Tang et al. 2011), laser (Liu et al. 2019), 3D printing (Elkholy and Kempers 2020) can also improve the surface heat transfer area and increase the nucleation sites by processing the micro-structures on the smooth surface. To sum up, the researchers can indeed enhance the heat transfer by processing the micro-nano structures to increase the heat transfer area and the number of nucleation sites. However, the micro-nano structures are usually located in the entire thermal boundary layer, which cannot give full play to the advantages of the micro-nano structures. The above variety of strengthening surface production methods is often expensive, and the long production period is not conducive to large-scale promotion and application. The critical heat flux (CHF) of these enhanced surfaces is usually less than 100 $W{\cdot}cm^{-2}$ for pool boiling experiments in a low saturated boiling point medium. In our previous work, large heat transfer enhancement area, controllable bubble generation and detachment frequency and good liquid supplement ability of pin–fin surface have been fully proved in the field of heat transfer enhancement (Cao et al. 2018, 2021; Liu et al. 2022a, b; Ma et al. 2009; Wei and Honda 2003; Yuan et al. 2020, 2009; Zhang et al. 2018a, b). Millimeter-scale mini-pin–fin has a relatively macro extended area that can break through the limitation of the thermal boundary layer and give full play to the heat transfer capacity of the extended area of the heat transfer surface.

In the present study, many millimeter-level mini-pin-finned copper surfaces with uniform distribution were manufactured. Compared with the surface of the micro-nano structures, it has a relatively macro extended area that can break through the limitation of the thermal boundary layer and give full play to the heat transfer capacity of the extended area of the heat transfer surface. We studied the effect of uniform mini pin-finned copper surfaces on the boiling heat transfer performance and the heat transfer efficiency in FC-72 fluid medium, observed the boiling phenomenon, and analyzed the heat transfer enhancement mechanism.

Experimental Apparatus and Procedure

Experimental Apparatus

The experimental apparatus, shown schematically in Fig. 1, consisted of four parts: the boiling chamber, temperature control system, data acquisition system, and the experimental modules (as shown in Fig. 2). The experimental module is composed of a cover plate and a heating base plate. The cover plate includes a mini-pin-finned copper surfaces, and the heating base plate includes a silicon wafer for heating. After assembling the cover plate and heating

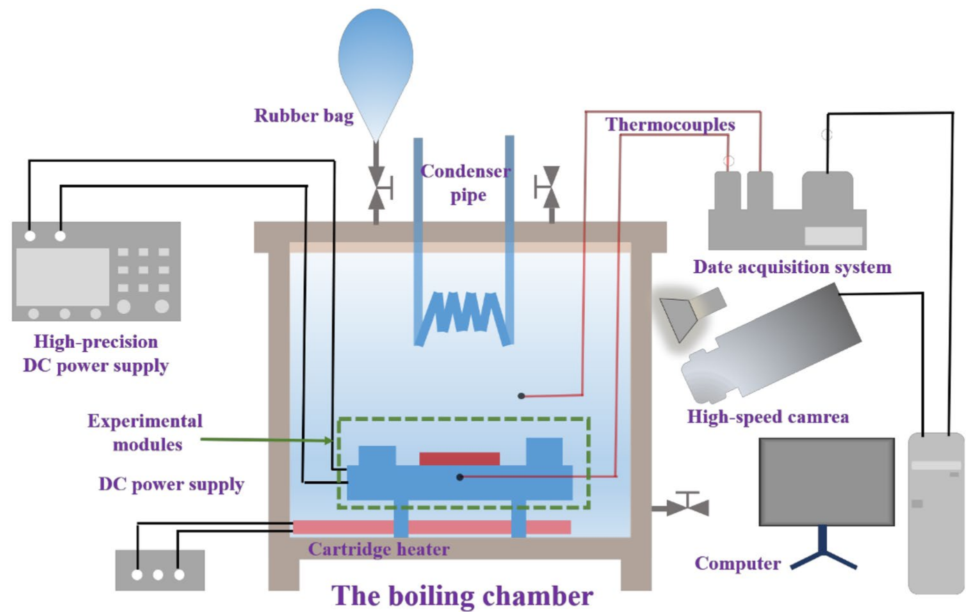

Fig. 1 Schematic diagram of the experimental system

the base plate separately, apply the proper amount of insulation glue between them and fix them together with bolts. The cubic boiling vessel that was filled with working fluids (approximately 1 L) was made of polymethyl methacrylate and had the dimensions of $100 \times 100 \times 100$ mm^3 in length, width, and height, respectively. The boiling chamber was washed with acetone, ethanol, and deionized water before loading into the working solution for using. A rubber bag with this volume of 3 L was used to maintain the pressure of the boiling vessel at 1 atm. An auxiliary heater with 200 W and a copper pipe was immersed in the working fluid to maintain the liquid subcooling of 0 K, 15 K, and 25 K (the saturated temperature of FC-72 is T_{sat} = 56 °C). The sealant was used to ensure the sealing of the entire boiling chamber. The FC-72 working liquid was commercially purchased from the 3 M corporation (USA) and stored according to standard storage conditions. The working fluid in the experiment don't removed non-condensable gases. In our previous study (Wei and Honda 2003), we have conducted the experiment to study the effects of degassed FC-72 and gas dissolved FC-72 on boiling heat transfer performance of micro-pin-finned surfaces. The results showed that at

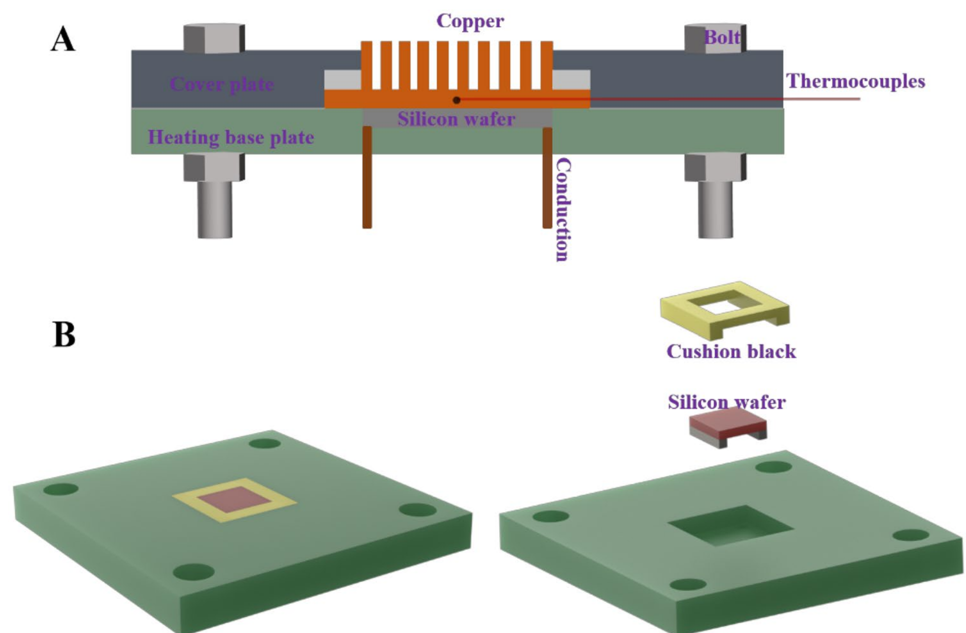

Fig. 2 The experimental modules. **A** Section view of the experimental module **B** Schematic diagram of the heating base plate

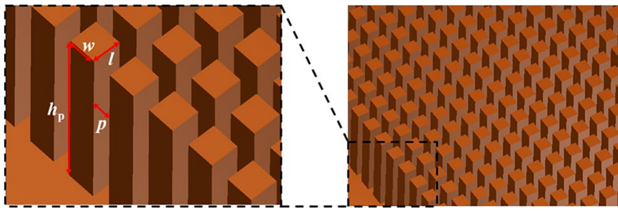

Fig. 3 Schematic diagram of uniform mini-pin-finned copper surface characteristic dimensions

low heat fluxes just after incipience, the dissolved air significantly enhances heat transfer but the effect diminishes with increasing heat flux similar to that observed for the flat surfaces and the microporous, square finned surfaces by Rainey et al. (Rainey et al. 2003). Thus, the air-dissolved FC-72 was used in the present study. A data acquisition instrument (cDAQ-9174, Power cord 240 W 10 A, NI 9212, USA) connected with a computer was used for the temperature collection. A high-speed digital camera (AOS corporation, Switzerland) with a lens (Computer MLM-3XMP) imaging 500 frame / s at a resolution of 1024 × 640 pixels was used for visualization.

Structural Design of Copper Surface

Uniform mini-pin-finned copper surface is mainly used to study the influence of several structural characteristics of the mini-pin–fin (including the height, spacing, and width) on the heat transfer performance. Their characteristic dimensions were shown in Fig. 3 and Table 1. Area enhancement ratio (A_{PF}/A_{SS}) was defined as the ratio of homogeneous mini-pin-finned copper surface area to smooth copper surface area, and it can represent the area enhancement factor of the uniformly distributed mini-pin-finned copper surface. It was calculated as follows:

$$\frac{A_{PF}}{A_{SS}} = \frac{(p+l)^2 + 4lh_p}{(p+l)^2} \tag{1}$$

The mini-pin-finned copper surface material is red copper, and the fin is processed by wire cutting. The thickness of the base of the experimental surface was 1.5 mm, the length and width were 13 mm, and the length and width of the heat transfer area were 10 mm. A hole with a diameter of 0.8 mm and a depth of 6.5 mm was machined in the center of the side of the base for installing thermocouples. The heated area was processed with copper pin fin array, the array of copper fin is different on different copper surfaces, and the rest was identical. The parameters of different copper surfaces were shown in the following table, take PF0.3–0.2–2 as an example, 0.3 means that the length(l) and width(w) of the mini-pin-fins are both 0.3 mm, 0.2 means that the fin pitch (p) between two mini-pin-fins is 0.2 mm, and 2 means that the height (h_p) of the mini-pin–fin was 2 mm. For the convenience of expression, surface PF is used in this paper to refer to mini-pin-finned copper surface. In addition, surface SS refers to the smooth copper surface.

Heat Flux and Uncertainty Analysis

The wall temperature error is caused by thermocouple calibration error (0.03 °C), temperature correction error from the bottom (0.2 °C), temperature fluctuation (0.1 °C) and thermocouple resolution (0.1 °C), which result in the total error of 0.25 °C calculated according to

$$\Delta T = \left(\Delta T_1^2 + T_2^2 + \cdots \Delta T_n^2\right)^{1/2}$$

The bulk liquid temperature error is 0.23 °C, which consists of thermocouple calibration error (0.03 °C), temperature fluctuation (0.1 °C) and thermocouple resolution (0.5 °C).

The input heat flux (q) of the heated silicon wafer could be calculated as follows:

$$q = \frac{U \cdot I}{a^2} \tag{2}$$

In the formula, U, I, and a are the heating voltage, heating current, and the length of the silicon wafer, respectively. And the uncertainty is:

Table 1 Characteristic dimensions of uniform mini-pin-finned copper surface

Surface	l (mm)	w (mm)	h_p (mm)	p (mm)	H_p/p	A_{PF}/A_{SS}
PF0.3–0.2–1	0.3	0.3	1	0.2	5.0	5.8
PF0.3–0.2–1.5	0.3	0.3	1.5	0.2	7.5	8.2
PF0.3–0.2–2	0.3	0.3	2	0.2	10	10.6
PF0.3–0.3–2	0.3	0.3	2	0.3	6.7	7.7
PF0.3–0.4–2	0.3	0.3	2	0.4	5.0	5.9
PF0.4–0.2–2	0.4	0.4	2	0.2	10	9.9
PF0.5–0.2–2	0.5	0.5	2	0.2	10	9.2
PF0.2–0.3–2	0.2	0.2	2	0.3	6.7	7.4
SS	/	/	/	/	/	/

$$\frac{\delta q}{q}=\left[\left(\frac{\delta U}{U}\right)^2+\left(\frac{\delta I}{I}\right)^2+2\left(\frac{\delta a}{a}\right)^2\right]^{1/2} \tag{3}$$

Heat loss (Δq_{loss}) is inevitable in the experiment. The heat loss of the system is mainly the heat loss of the conduction wires on both sides of the silicon wafer and the heat transfer loss of the epoxy resin in the experimental module, and it can be calculated as follows:

$$\frac{\delta q_{all}}{q}=\frac{\delta q}{q}+\frac{\Delta q_{loss}}{q}=\left[\left(\frac{\delta U}{U}\right)^2+\left(\frac{\delta I}{I}\right)^2+2\left(\frac{\delta a}{a}\right)^2\right]^{1/2}+\frac{\Delta q_{loss}}{q} \tag{4}$$

The uncertainties of U, I and a are 0.01%, 0.1% and 0.5%, respectively. Previous research (O'Connor and You 1995) has shown that the heat loss is 15.5% in the natural convective heat transfer region, while in the nucleate boiling heat transfer region, the heat loss was 5.0%. Considering that the mini-pin-finned surface has the function of strengthening heat transfer and the heat loss is smaller, so the total heat loss adopted above results are credible. After comprehensive consideration, the uncertainty of the forced convective heat transfer region is 16%, and the uncertainty of the nuclear boiling heat transfer region is 6%.

Results and Discussion

The Effect of Mini-pin–fin Height

The effect of mini-pin–fin height on the heat transfer performance is shown in Fig. 4. Here, only the height of mini-pin–fin on the surface PF0.3–0.2–1, PF0.3–0.2–1.5, and

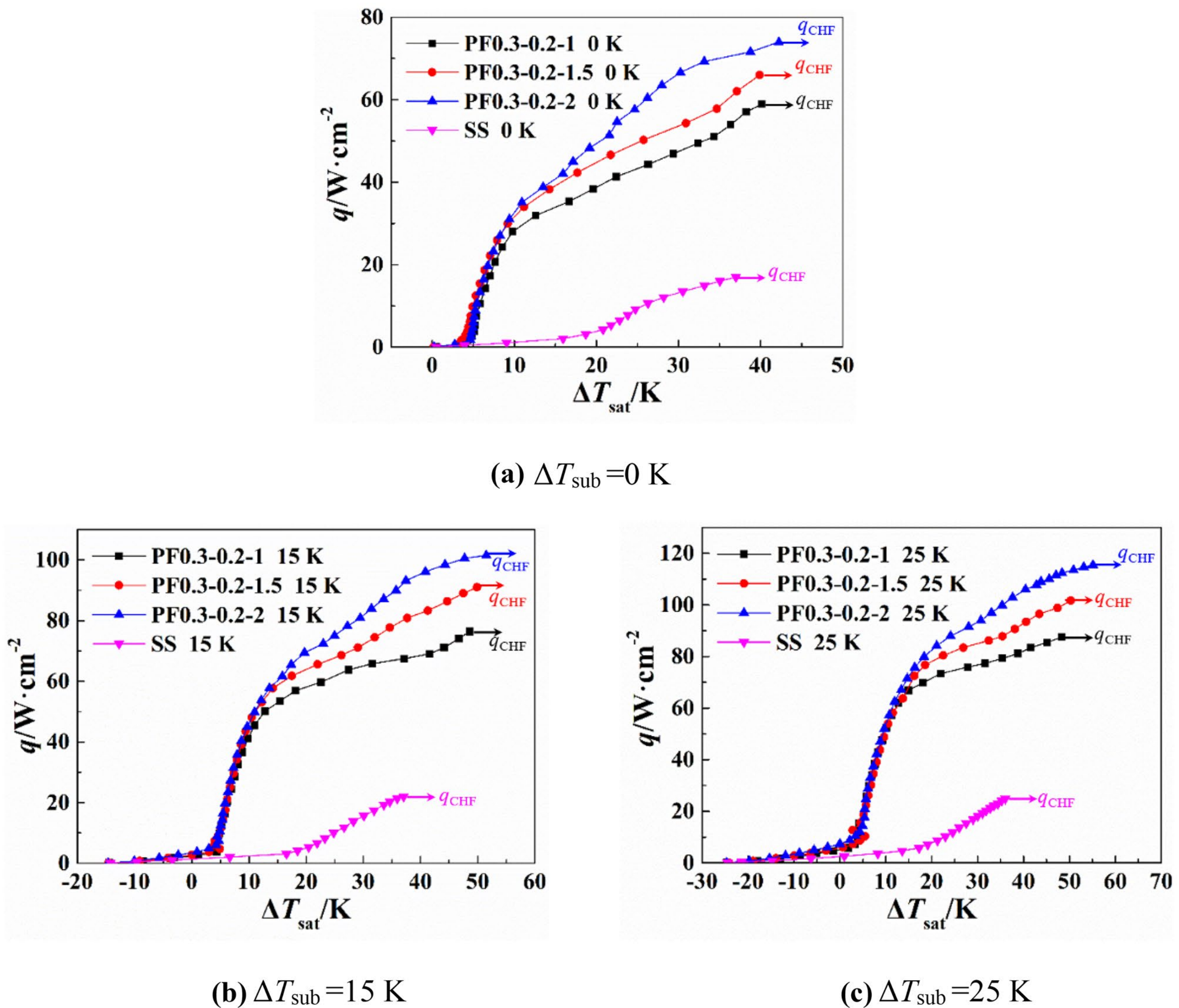

Fig. 4 The influence of copper fin height on the copper surface boiling curve

PF0.3–0.2–2 are different. In addition, the other parameters of the three surfaces are the same, and the surface SS is used as the control group.

The boiling curves at low and medium heat fluxes were coincident and the coincidence part of the boiling curve increased with increasing subcooling. The reasons are as follows. The liquid subcooling $\Delta T_{sub} = 0$ K meant that the cooling medium was at a saturation temperature. The heat exchange between the lower part of the mini-pin-fins and the main cooling medium in the boiling pool was fewer, which caused the cooling medium around the lower part of the mini-pin-fins to overheat firstly and generated bubbles generating from the lower part of the copper pin-fins and the upper surface of the copper substrate in the low heat fluxes. But the cooling medium on the upper part of the mini-pin-fins was relatively close to the main cooling medium and the heat exchange was relatively larger. As the subcooling increased, the temperature of the cooling medium gradually decreased and the temperature difference between the cooling medium at the lower part of the mini-pin-fins and the main cooling medium increased. The bigger temperature difference meant the heat required for the cooling medium to reach the superheated state to activate the nucleation sites increased. This might provide support for the fact that the coincidence part of the boiling curve increased with increasing subcooling.

The CHF on the copper surface increased with the fin height at the same liquid subcooling condition. At high heat fluxes, the higher the fin height, the more the boiling curve slopes upward and the greater the CHF. This indicated that the contribution of the increased fin height to enhanced heat transfer was more pronounced at high heat fluxes. As shown in Fig. 4, when liquid subcooling ΔT_{sub} was 0 K, 15 K, and 25 K, the maximum heat flux of coincidence of different surface boiling curves was about 25 W·cm^{-2}, 50 W·cm^{-2}, and 75 W·cm^{-2}, respectively. The following description may provide support. The lower part of the mini-pin-fins and the upper surface of the copper base was in the nucleate boiling region, we defined it as the main boiling zone; the upper part of the mini-pin-fins was mostly in the natural convection stage or the boiling stage with different degrees of boiling intensity, which defined as the secondary boiling zone, as shown Fig. 5. The area of the main boiling zone on copper surfaces at different fin-heights was approximately equal at low heat flux and the height of the fin has essentially no effect on the heat transfer performance, which might explain the almost coincidence of the boiling curves of the three surfaces at medium and low heat fluxes. However, the effect of the fin-height on the heat transfer performance was shown at medium to high heat fluxes. The temperature of the cooling medium around the entire mini-pin-fins was higher and it was in a state of overheating. The more nucleation sites of the secondary boiling zone on the copper surface were activated. Meanwhile, the enhanced natural convection made the fresh liquid on the surface of the pin–fin more replenished. The larger the fin height, the greater the effect of the sub-boiling zone, and the greater the CHF. When liquid subcooling ΔT_{sub} was 25 K, The CHF of PF0.3–0.2–2 increased by 362% compared to the smooth copper surface.

To further explore the effect of the fin-height on the boiling heat transfer performance, the HTC of copper surfaces of different fin-height was investigated, as shown in Fig. 6. Compared to the smooth copper surface, all three surfaces showed a greater improvement in HTC at different subcooling. Specifically, the liquid subcooling $\Delta T_{sub} = 0$ K, the major boiling zones at low heat flux were essentially the same and the HTC was essentially the same. The boiling heat transfer area of PF0.3–0.2–2 was the largest and HTC was the largest at medium to high heat fluxes. The influence of the three copper surfaces on HTC was similar to 0 K, when the liquid subcooling was15 K and 25 K. The HTC was almost the same at medium heat fluxes because of the similar boiling heat transfer area of main boiling area.

The Effect of Mini-pin–fin Spacing

The effect of mini-pin–fin spacing on the heat transfer performance is shown in Fig. 7. Here, only the spacing of mini-pin–fin on the surface PF0.3–0.4–2, PF0.3–0.3–2 and PF0.3–0.2–2 are different. In addition, the other parameters of the three surfaces are the same, and the surface SS is used as the control group.

The CHF on the copper surface increased with the decrease of the fin spacing at the same liquid subcooling condition. The boiling curves of PF0.3–0.4–2 and PF0.3–0.3–2 were almost perfectly coincident at low and medium heat fluxes. The boiling curve of PF0.3–0.2–2 had an overall shift to the upper left in the medium to high heat fluxes with respect to the

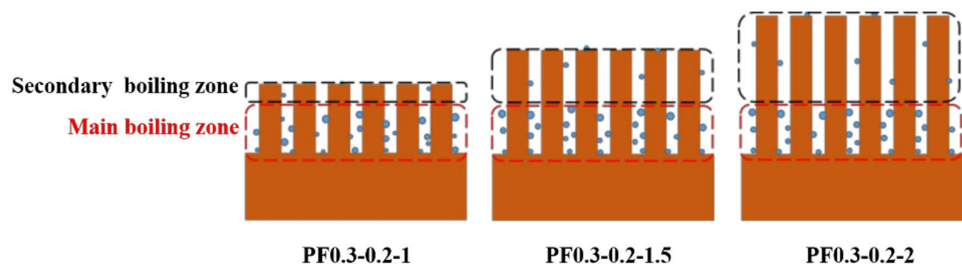

Fig. 5 Schematic diagram of the boiling area on the copper surface in low and to medium heat fluxes

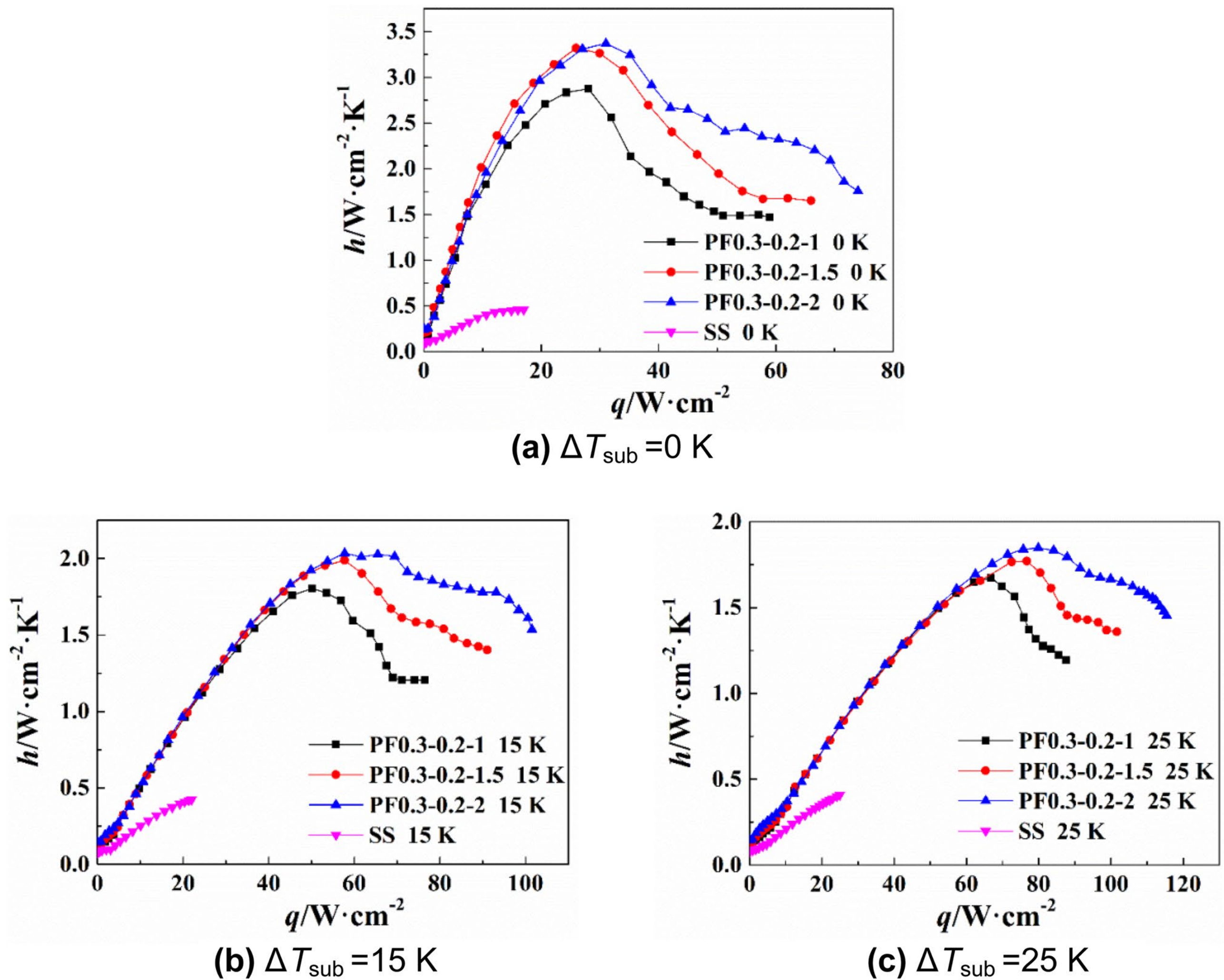

Fig. 6 The influence of copper fin height on copper surface HTC

other two boiling curves. Which indicated the improvement of surface boiling heat transfer would be more obvious when the fin spacing was reduced to 0.2 mm.

Concretely, when the liquid subcooling was 0 K ($\Delta T_{sub} = 0$ K), the temperature of the working medium was higher. The boiling curves of the different surfaces almost coincided because they were both in the unidirectional convection phase at low heat fluxes. The bubbles started to be generated at middle heat fluxes, the fin spacing of PF0.3–0.2–2 was smaller than the other two copper surfaces, which could limit the radius of the bubbles and increase departure frequency. Meanwhile, the surface had the largest heat transfer area and could provide a large number of nucleation sites, which improved the heat transfer performance. Although the heat transfer area of PF0.3–0.4–2 was the smallest (the fin spacing was the largest), the liquid replenishment on the copper surface was more sufficient. The sufficient liquid replenishment might explain the comparable heat transfer capacity of PF0.3–0.4–2 and PF0.3–0.3–2 at middle heat fluxes. At high heat fluxes, the heat exchange of the cooling medium between the copper fin and the main cooling medium was very sufficient, and the copper surface heat transfer area played a decisive role in improving the heat transfer performance. As was shown in Table 1, the area enhancement ratio of PF0.3–0.2–2 was the biggest of the three copper surfaces, so it had the best heat transfer performance. The boiling curves at 15 K and 25 K were similar to 0 K.

As shown in Fig. 8, the HTC of all three surfaces had improved considerably compared to the SS surface. The HTC of PF0.3–0.2–2 was larger than the other two surfaces at low heat fluxes.

With the continuous growth of the bubble, when the diameter of the bubble increases to a certain extent, it will be detached from the heating surface under the action of the normal force, especially the buoyancy. At this time, the diameter of the bubble is the detachment diameter.

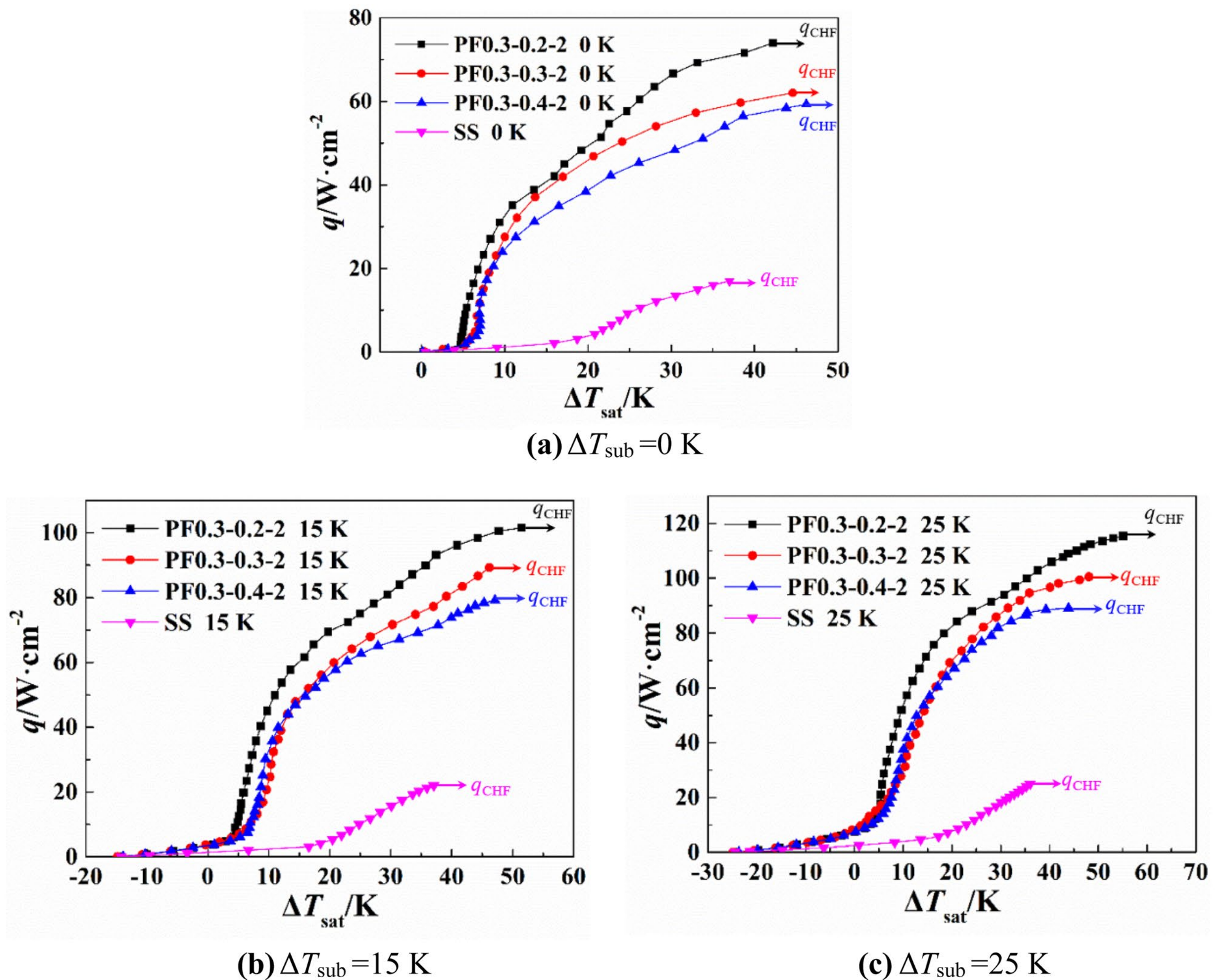

Fig. 7 The influence of copper fin spacing on the copper surface boiling curve

The bubbles with larger detachment diameters is easy to merge with its surrounding bubbles to form a vapor film to deteriorate heat transfer. Our previous work on bubble behavior of micro-pin-finned surfaces found the smaller the pin–fin spacing, the earlier the bubbles can contact the side of the pin–fin. Under the influence of pin–fin wall heat transfer, the growth and detachment rate of bubbles is faster (Zhou et al. 2020, 2022). On the other hand, the pinning effect of the microstructure surface also promotes the increase in the frequency of bubble detachment (Jo et al. 2016; Liu et al. 2018, 2020). So, PF0.3–0.2–2 had a smaller copper fin spacing, bubble departure radius, and higher bubble departure frequency. Meanwhile, the surface had the largest heat transfer area and could provide a large number of nucleation sites, which improved the HTC of the copper surface. The large number of bubbles on the copper surface at medium to high heat fluxes resulted in stronger disturbance behavior. Heat transfer performance was mainly determined by the area of the heat transfer surface and the HTC of PF0.3–0.2–2 was the biggest.

The Effect of the Mini-pin–fin Width

The effect of mini-pin–fin width on the heat transfer performance is shown in Fig. 9. Here, only the width of mini-pin–fin on the surface PF0.5–0.2–2, PF0.4–0.2–2, and PF0.3–0.2–2 are different. In addition, the other parameters of the three surfaces are the same, and the surface SS is used as the control group.

The copper surface at low heat fluxes was in the single-phase natural convection stage, and the boiling curves almost overlapped. As the heat fluxes increased, bubbles began to form on the copper surface and the heat exchange of the cooling medium between the copper fin and the main cooling

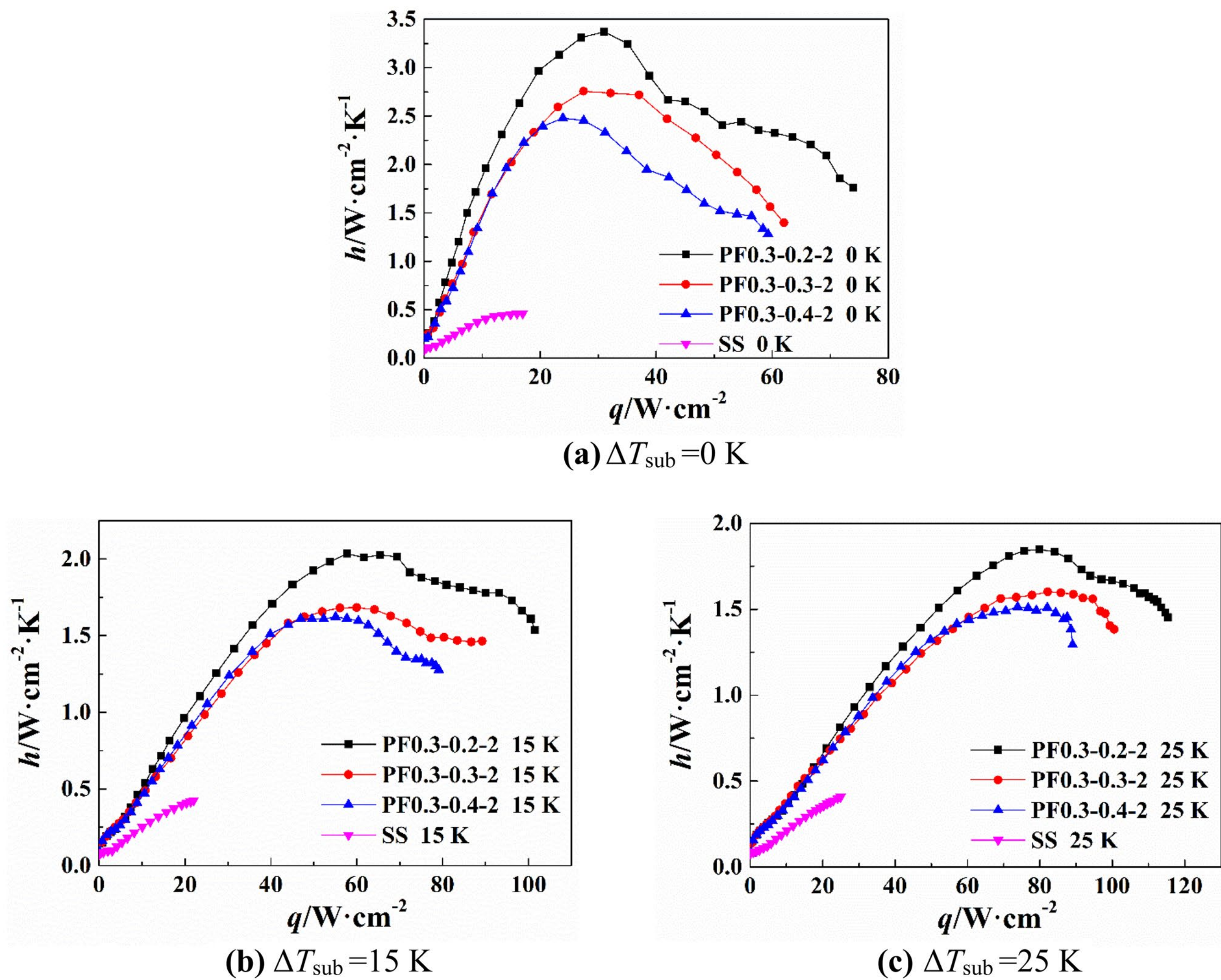

Fig. 8 The influence of copper fin spacing on copper surface HTC

medium was more sufficient. The increase in the fin width meant that the number of copper fins decrease, the fewer copper fin meant that the surface area of copper became smaller, so the heat transfer performance of PF0.5–0.2–2 was the worst.

The HTC of all three surfaces had improved considerably compared to the SS surface, as shown in Fig. 10. HTC overlapped at low heat fluxes, and the copper surface was in the natural convection phase at this time. The heat transfer performance at medium to high heat fluxes depended on the area of the copper surface, so the larger the fin width, the worse the heat transfer performance. However, when the subcooling increased, the temperature difference between the cooling working medium and the copper surface increased. The greater temperature difference promoted the heat dissipation from the copper surface. Although the surface areas of different surfaces were different, they had a nearly similar HTC at medium heat fluxes.

Boiling Phenomenon on the Mini-pin-finned Surfaces

The bubble behavior on the copper surface was researched by high-speed camera, as shown in Fig. 11. There were similarities in the behavior of vapor bubbles on different surfaces, from single-phase natural convection, to the generation of a small number of tiny bubbles, to the generation of a large number of tiny bubbles, and finally to the merger of tiny bubbles into a large bubble process. At high heat fluxes, the vapor bubbles merged to form a vapor cloud and wrapped around the entire copper surface. The decrease of contact between the copper surface and main cooling medium affects the further increase of HTC and CHF. Specifically, taken PF0.3–0.2–1 as an example to illustrate. A little number of vapor bubbles were generated on the copper surface and the activated nucleation sites were also few at $q = 6$ W·cm^{-2}. Bubbles and nucleation sites gradually increased at $q = 10$

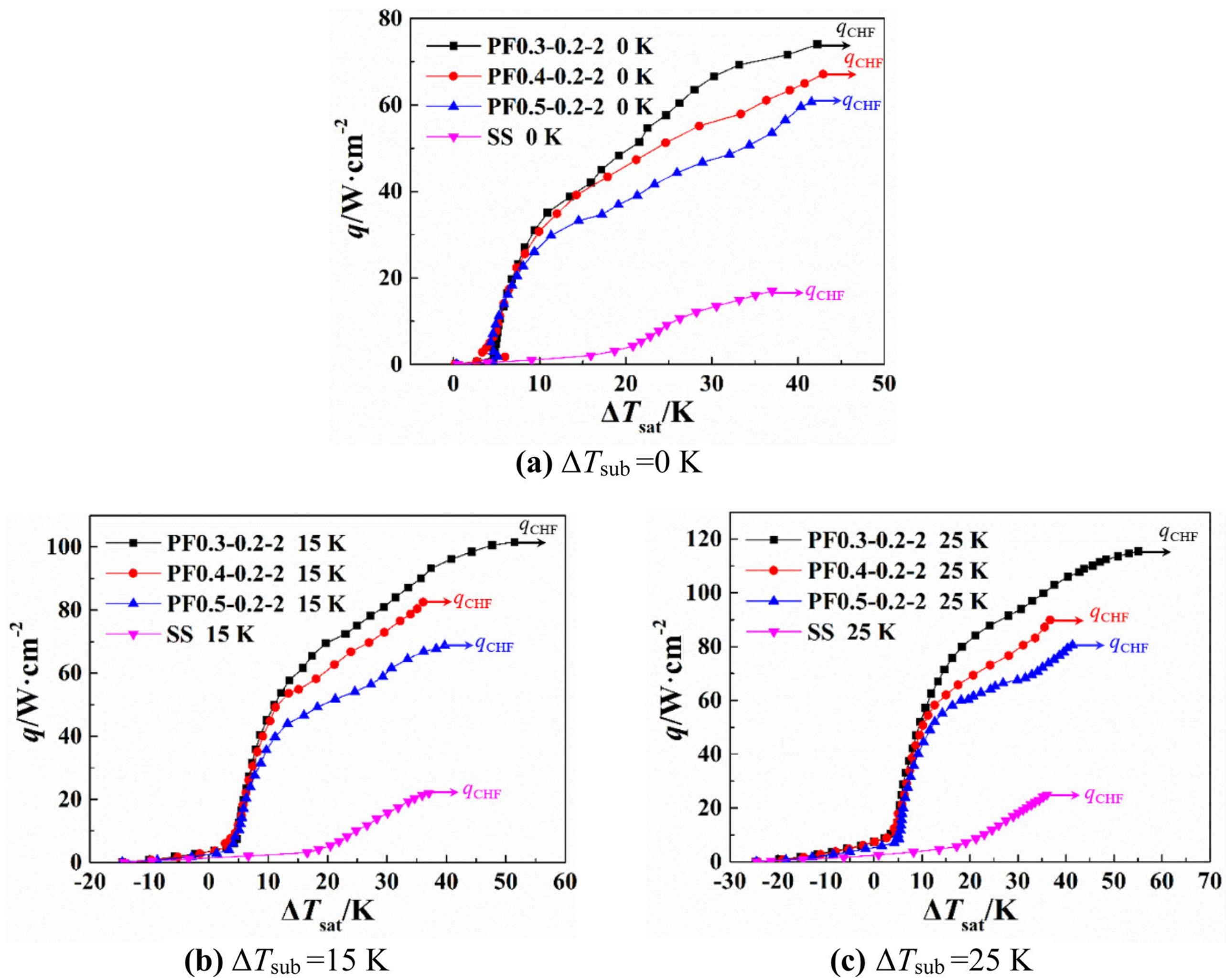

Fig. 9 The influence of copper fin width on the copper surface boiling curve

W·cm^{-2}. When the heat flux reached 30 W·cm^{-2}, a large number of tiny bubbles appeared on the copper surface and quickly separated from the surface and the bubbles took away massive heat. The HTC reached maximum value due to all vaporized cores being activated. As the heat fluxes increased further (q = 30 W·cm^{-2}), large bubbles covered part of the copper surface. As the copper surface lacked the recharge of the cooling working medium at this time, HTC became smaller. A large vapor bubble adhered to the entire copper surface, which creates a great obstacle to the recharge of fresh cooling working medium on the copper surface at q = 80 W·cm^{-2}, and the HTC of the copper surface further decreased.

Bubble departure showed a periodic pattern at high heat flux, as shown in Fig. 12.

First, several small bubbles form on the copper surface (Fig. 12a); Subsequently, small bubbles merge into irregular large bubbles (Fig. 12b); With the continuous increase of the volume of the large bubbles, the contact between the copper surface and the bottom of the large bubbles became less and less, and finally, the bubbles were separated from the copper surface (Fig. 12c).

Mini-pin–fin Efficiency

To characterize the effective degree of heat dissipation of the mini-pin-finned surfaces, the fin efficiency is introduced for analysis, and it could be calculated as follows:

$$\eta_f = \frac{tanh\left[\sqrt{\frac{2h}{\lambda w}}\left(h_p + w/2\right)\right]}{\sqrt{\frac{2h}{\lambda w}}\left(h_p + w/2\right)} \quad (5)$$

where h is the HTC between copper mini-pin-fins and working medium (W·m^{-2} K^{-1}). λ is the thermal conductivity of

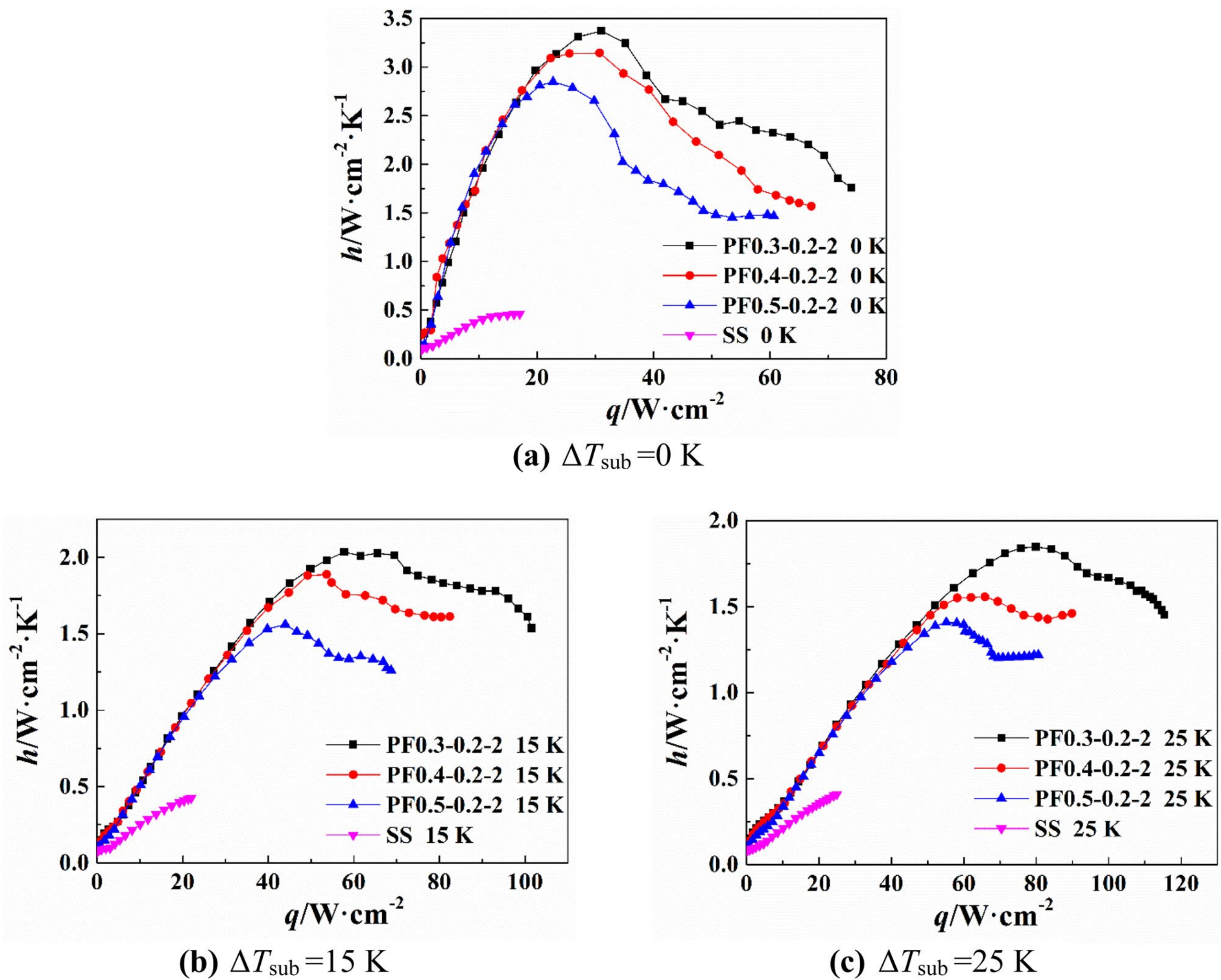

Fig. 10 The influence of fin width on copper surface HTC

copper mini-pin-fins (W·m^{-1}·K^{-1}). h_p is the height of the mini-pin-fins(mm).w is the width of the mini-pin-fins(mm).

Mini-pin–fin efficiency $\left(\eta_f\right)$ represents the ratio of the actual heat dissipation of the copper fin to the heat dissipation when the entire copper surface is assumed to be at the bottom temperature of the copper fin. The larger the efficiency of the copper fin, the more conducive to the heat dissipation of the copper surface. The mini-pin-finned copper surfaces were studied in this paper involve many variations in height, spacing, and width, all of which had an effect on copper mini-pin–fin efficiency, as shown in Fig. 13. Investigating the effects of different factors on the mini-pin–fin efficiency could guide to provide designers with design solutions that could improve mini-pin–fin efficiency.

For PF0.3–0.2–1, PF0.3–0.2–1.5, and PF0.3–0.2–2 with gradually increasing height of mini-pin-fins, the fin efficiency increased with increasing height of mini-pin-fins at the same heat flux. The fin height directly affected the heat transfer area, the higher the height, the larger the heat transfer area. For PF0.3–0.2–2, PF0.3–0.3–2, PF0.3–0.4–2 with gradually increasing copper fin spacing, the copper fin efficiency increased with increasing copper fin spacing at the same heat flux. The larger spacing between the fins could accommodate more cooling working medium, which allowed the upper and lower parts of the fins to have more contact area with the cooling working medium. This made a more uniform temperature distribution throughout the fins. For copper fin width gradually increasing PF0.3–0.2–2, PF0.4–0.2–2 and PF0.5–0.2–2, at the same heat flux, the copper fin efficiency increased with the increase of the fin width. This was determined by the material of the copper fins, the copper itself had very good thermal conductivity, with the increase of the fin width, the cross-sectional area of the copper fins increases, the internal temperature distribution of the copper fins more

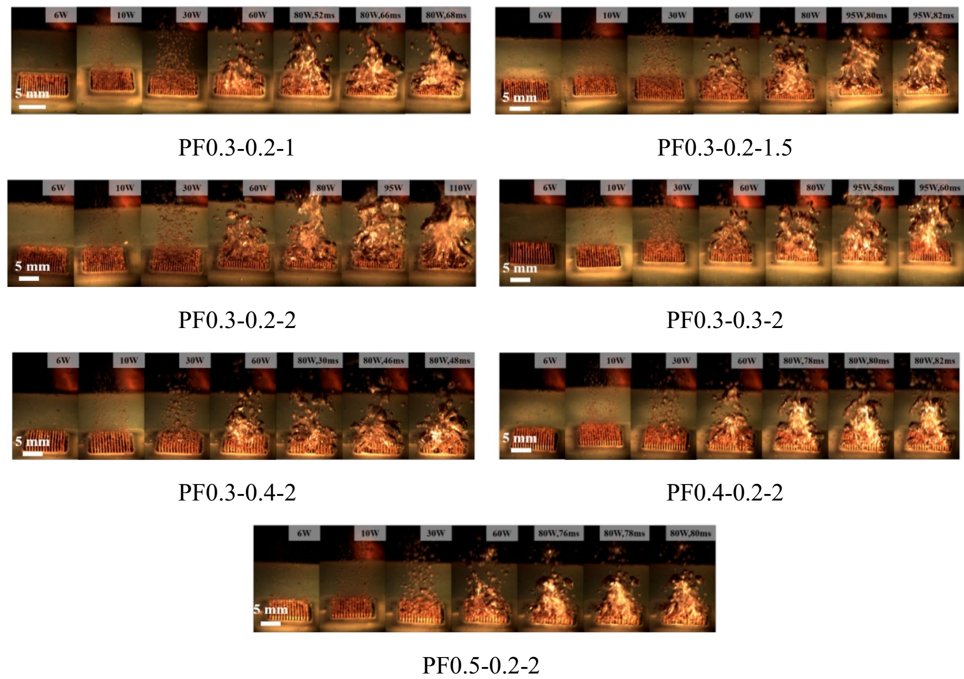

Fig. 11 Vapor bubble behavior at different heat flux (ΔT_{sub} = 25 K)

uniform, so that the average temperature of the entire surface of the copper fins was closer to the temperature of the lower part of the copper fins, which led to higher fin efficiency.

The copper fin height, spacing, and width had an impact on the fin efficiency of the copper surface. As shown in Fig. 13, the fin efficiency of PF0.3–0.2–2 was not the highest, but its CHF was the largest. The largest area enhancement ratio of PF0.3–0.2–2 could provide the largest heat transfer area and made up for the disadvantage of the lower fin efficiency on this surface. Hence, it suggested that it was more beneficial to increase the heat transfer area enhancement ratio of the uniform mini-pin-finned copper surface to increase the CHF. When the height of the mini-pin-fins was the same, increasing the fin spacing and the fin width could improve the fin efficiency, but the improvement was limited. In comparison, the fin height had a greater contribution to the fin efficiency and

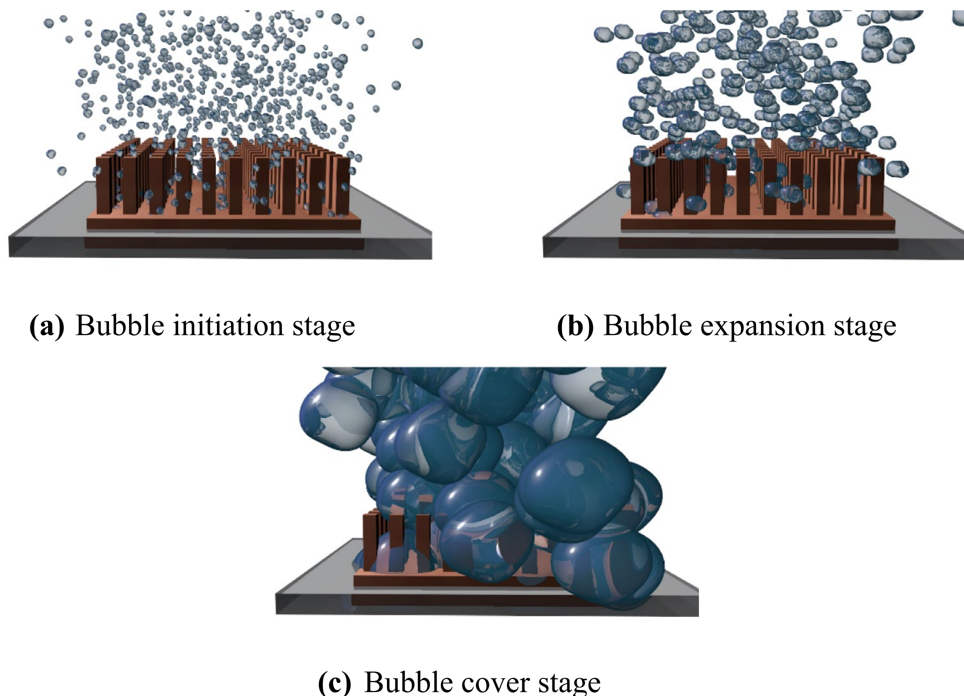

Fig. 12 Schematic diagram of bubble boiling on copper surface

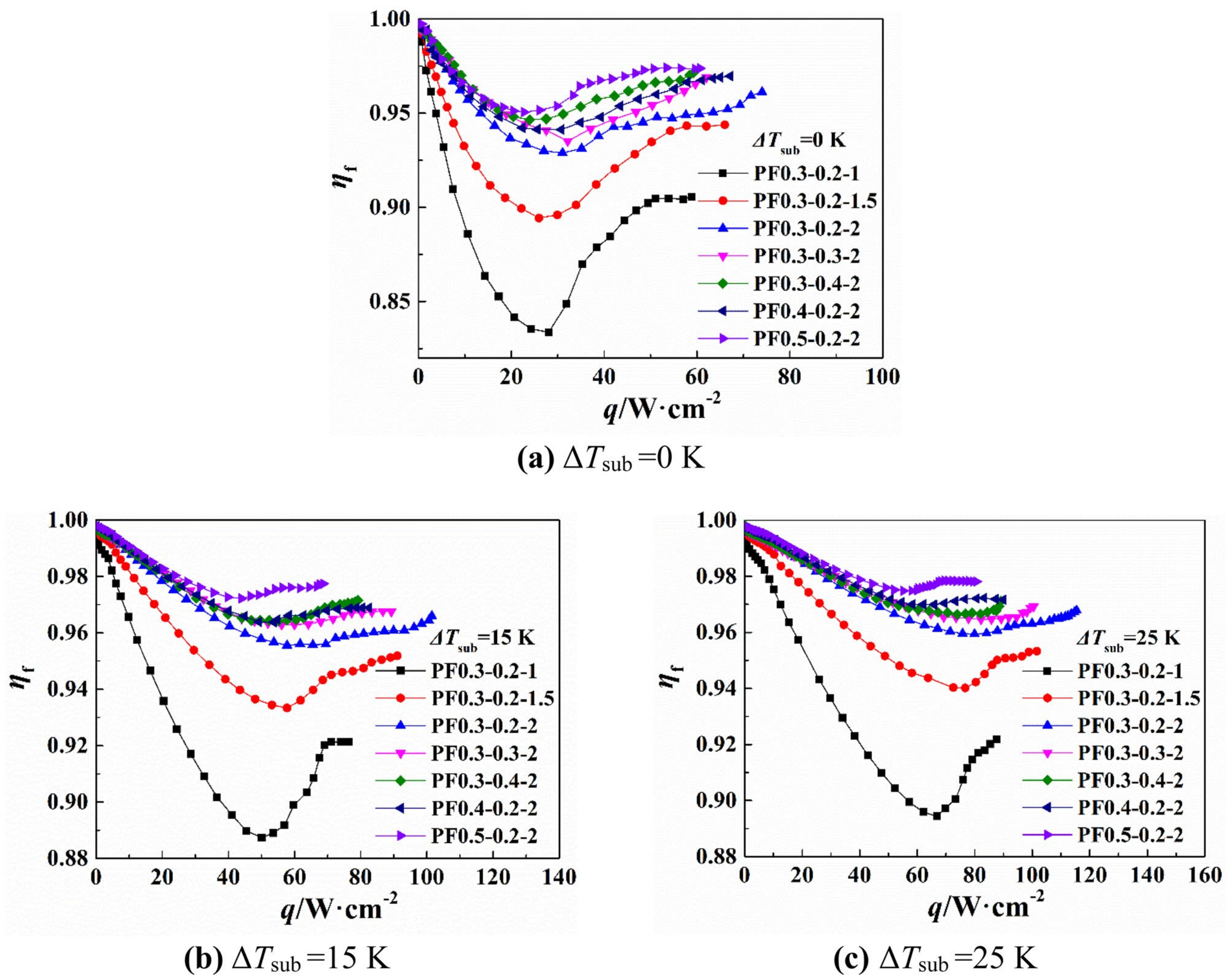

Fig. 13 The effect of the height, spacing, and width of copper fin on the fin efficiency

played a leading role in improving the fin efficiency. For the copper surfaces with similar heat transfer area enhancement ratio (such as PF0.3–0.2–1 ($A_{PF}/A_{SS} = 5.8$) and PF0.3–0.4–2 ($A_{PF}/A_{SS} = 5.9$), PF0.3–0.3–2 ($A_{PF}/A_{SS} = 7.7$) and PF 0.3–0.2–1.5 ($A_{PF}/A_{SS} = 8.2$)), the fin efficiency increased with the increasing of the fin height and spacing. When designing the copper surface, the fin height and spacing of the copper surface could be increased as large as possible to improve the fin efficiency, but the premise was that the heat transfer area enhancement ratio did not vary much.

Conclusions

In this paper, we conducted several pool boiling experiments of mini-pin-finned copper surface with multiple subcooling degrees, analyzed several factors affecting the heat transfer performance and the boiling phenomenon at high heat flux. The following conclusions can be obtained.

1. The CHF and HTC of the uniform mini-pin-finned copper surfaces increased with the increase of subcooling. At the same liquid subcooling, the CHF and HTC of uniform mini-pin-finned copper surfaces increased with increasing fin height, decreased with increasing fin spacing and width. The CHF of PF0.3–0.2–2 reached 115.4 W·cm^{-2} at $\Delta T_{sub} = 25$ K, which was about 3.6 times higher than that of the smooth copper surface.
2. The behavior of vapor bubbles on the different uniform mini-pin-finned copper surfaces was relatively similar, and they all go through the process from single-phase natural convection, to the generation of a small number of tiny vapor bubbles, to the generation of a large number of tiny vapor bubbles, and finally to the merging of tiny vapor bubbles into large vapor bubbles.

3. At the same liquid subcooling, the efficiency of mini-pin-fins on the copper surface increased with the increase of fin height, spacing, and width. To improve the CHF of the mini-pin-fined copper surface, it is necessary to balance the heat transfer area enhancement ratio and the mini-pin–fin efficiency. When designing the copper surface, the height and spacing of the mini-pin-fins can be as large as possible, which could significantly improve the efficiency of the mini-pin-fins, provided that the heat transfer area enhancement ratio did not vary much.

Nomenclature A: Surface area of a silicon wafer(cm^2); A_{PF}: Surface area of the uniform mini-pin-finned copper surfaces(cm^2); A_{SS}: Surface area of smooth copper surface(cm^2); A: Length of silicon wafer (mm); h_p: Height of copper mini-pin-fins(mm); l: Length of copper mini-pin-fins (mm); p: Spacing of copper mini-pin-fins (mm); w: Width of copper mini-pin-fins (mm); P: Power(W); h(HTC): Boiling heat transfer coefficient($W \cdot m^{-2} \cdot K^{-1}$); CHF: Critical heat flux ($W \cdot m^{-2}$); U: Heating voltage(V); I: Heating current(A); q: Heat flux ($W \cdot m^{-2}$); T: Temperature(K); ΔT: Temperature difference(K); η_f: Mini-pin–fin Efficiency; T_f: Liquid temperature(K); Max: Maximum; T_{sat}: Saturated temperature(K); T_{sub}: Subcooling temperature(K).

Funding This work is supported by the National Natural Science Foundation of China (No. 51976163), Key research and development program in Shaanxi Province of China (No.2021GXLH-Z-076), Joint Funds of the National Natural Science Foundation of China (No.U2141218, U1738119), Second batch of scientific experiment proposals aboard China Space Station (No.TGMTYY00-JY-53–1.00), and ESA-CMSA Joint Boiling Project (No.TGMTYY00-RW-05–1.00).

Declarations

Competing Interest The authors declare that they have no known competing financial interests or personal relationships that could have appeared to influence the work reported in this paper.

References

Adeoye, S., Parahovnik, A., Peles, Y.: A micro impinging jet with supercritical carbon dioxide. Int. J. Heat. Mass. Transf. **170**, 121028 (2021)

Bar-Cohen, A., Wang, P.: On-chip Hot Spot Remediation with Miniaturized Thermoelectric Coolers. Microgravity Sci. Technol. **21**(S1), 351–359 (2009)

Bertossi, R., Caney, N., Gruss, J.A., Dijon, J., Fournier, A., Marty, P.: Influence of carbon nanotubes on deionized water pool boiling performances. Exp. Thermal. Fluid Sci. **61**, 187–193 (2015)

Byon, C., Choi, S., Kim, S.J.: Critical heat flux of bi-porous sintered copper coatings in FC-72. Int. J. Heat. Mass. Transf. **65**, 655–661 (2013)

Cao, Z., Liu, B., Preger, C., Wu, Z., Zhang, Y., Wang, X., Messing, M.E., Deppert, K., Wei, J., Sundén, B.: Pool boiling heat transfer of FC-72 on pin-fin silicon surfaces with nanoparticle deposition. Int. J. Heat. Mass. Transf. **126**, 1019–1033 (2018)

Cao, Z., Liu, B., Preger, C., Zhang, Y.H., Wu, Z., Messing, M.E., Deppert, K., Wei, J.J., Sundén, B.: Nanoparticle-Assisted Pool Boiling Heat Transfer on Micro-Pin-Fin Surfaces. Langmuir **37**(3), 1089–1101 (2021)

Dadjoo, M., Etesami, N., Esfahany, M.N.: Influence of orientation and roughness of heater surface on critical heat flux and pool boiling heat transfer coefficient of nanofluid. Appl. Therm. Eng. **124**, 353–361 (2017)

Devahdhanush, V.S., Mudawar, I.: Review of Critical Heat Flux (CHF) in Jet Impingement Boiling. Int. J. Heat. Mass. Transf. **169**, 120893 (2021)

Dhadda, G., Hamed, M., Koshy, P.: Electrical discharge surface texturing for enhanced pool boiling heat transfer. J. Mater. Process. Technol. **293**, 117083 (2021)

Duan, L., Liu, B., Qi, B., Zhang, Y., Wei, J.: Pool boiling heat transfer on silicon chips with non-uniform micro-pillars. Int. J. Heat. Mass. Transf. **151**, 119456 (2020)

Elkholy, A., Kempers, R.: Enhancement of pool boiling heat transfer using 3D-printed polymer fixtures. Exp. Thermal. Fluid. Sci. **114**, 110056 (2020)

Fan, S., Jiao, L., Wang, K., Duan, F.: Pool boiling heat transfer of saturated water on rough surfaces with the effect of roughening techniques. Int. J. Heat. Mass. Transf. **159**, 120054 (2020)

Godinez, J.C., Cho, H., Fadda, D., Lee, J., Park, S.J., You, S.M.: Effects of materials and microstructures on pool boiling of saturated water from metallic surfaces. Int. J. Therm. Sci. **165**, 106929 (2021)

Gupta, S.K., Misra, R.D.: Flow boiling heat transfer performance of copper-alumina micro-nanostructured surfaces developed by forced convection electrodeposition technique. Chem. Eng. Process. Process. Intensif. **164**, 108408 (2021)

He, Z., Yan, Y., Zhang, Z.: Thermal management and temperature uniformity enhancement of electronic devices by micro heat sinks: A review. Energy **216**, 119223 (2021)

Jo, H., Park, H.S., Kim, M.H.: Single bubble dynamics on hydrophobic–hydrophilic mixed surfaces. Int. J. Heat. Mass. Transf. **93**, 554–565 (2016)

Jothi Prakash, C.G., Prasanth, R.: Enhanced boiling heat transfer by nano structured surfaces and nanofluids. Renew. Sustain. Energy. Rev. **82**, 4028–4043 (2018)

Jung, J.-Y., Kwak, H.-Y.: Effect of surface condition on boiling heat transfer from silicon chip with submicron-scale roughness. Int. J. Heat. Mass. Transf. **49**(23–24), 4543–4551 (2006)

Kim, B.S., Lee, H., Shin, S., Choi, G., Cho, H.H.: Interfacial wicking dynamics and its impact on critical heat flux of boiling heat transfer. Appl. Phys. Lett. **105**(19), 191601 (2014)

Kim, J.M., Kong, B., Lee, H.-B.-R., Wongwises, S., Ahn, H.S.: Effect of h-BN coating on nucleate boiling heat transfer performance in pool boiling. Exp. Therma.l Fluid. Sci. **98**, 12–19 (2018)

Kim, S.H., Lee, G.C., Kang, J.Y., Moriyama, K., Kim, M.H., Park, H.S.: Boiling heat transfer and critical heat flux evaluation of the pool boiling on micro structured surface. Int. J. Heat. Mass. Transf. **91**, 1140–1147 (2015)

Kim, Y.C.: Effect of surface roughness on pool boiling heat transfer in subcooled water-CuO nanofluid. J. Mech. Sci. Technol. **28**(8), 3371–3376 (2014)

Kong, X., Zhang, Y., Wei, J.: Experimental study of pool boiling heat transfer on novel bistructured surfaces based on micro-pin-finned structure. Exp. Thermal. Fluid Sci. **91**, 9–19 (2018)

Lee, J., Mudawar, I.: Fluid flow and heat transfer characteristics of low temperature two-phase micro-channel heat sinks – Part 1: Experimental methods and flow visualization results. Int. J. Heat. Mass. Transf. **51**(17–18), 4315–4326 (2008)

Li, C.H., Li, T., Hodgins, P., Hunter, C.N., Voevodin, A.A., Jones, J.G., Peterson, G.P.: Comparison study of liquid replenishing impacts

on critical heat flux and heat transfer coefficient of nucleate pool boiling on multiscale modulated porous structures. Int. J. Heat. Mass. Transf. **54**(15–16), 3146–3155 (2011)

Li, H., Li, R., Zhou, R., Zhou, G., Tang, Y.: Pool boiling heat transfer of multi-scale composite copper powders fabricated by sintering-alloying-dealloying treatment. Int. J. Heat. Mass. Transf. **147**, 118962 (2020)

Li, J.-Q., Mou, L.-W., Zhang, Y.-H., Yang, Z.-S., Hou, M.-H., Fan, L.-W., Yu, Z.-T.: An experimental study of the accelerated quenching rate and enhanced pool boiling heat transfer on rodlets with a superhydrophilic surface in subcooled water. Exp. Thermal. Fluid Sci. **92**, 103–112 (2018)

Li, K., Zhao, J.-F., Kang, Q., Wang, S.-F.: Academician Wen-Rui Hu – Eminent Pioneer and Prominent Leader of Microgravity Science in China. Microgravity. Sci. Technol. **34**(2) (2022)

Liang, G., Mudawar, I.: Review of nanoscale boiling enhancement techniques and proposed systematic testing strategy to ensure cooling reliability and repeatability. Appl. Therm. Eng. **184**, 115982 (2021)

Liu, B., Cao, Z., Zhang, Y., Wu, Z., Pham, A., Wang, W., Yan, Z., Wei, J., Sundén, B.: Pool boiling heat transfer of N-pentane on micro/nanostructured surfaces. Int. J. Therm. Sci. **130**, 386–394 (2018)

Liu, B., Garivalis, A.I., Cao, Z., Zhang, Y., Wei, J., Marco, P.D.: Effects of electric field on pool boiling heat transfer over microstructured surfaces under different liquid subcoolings, Int. J. Heat. Mass. Transf. **183** (2022a)

Liu, B., Liu, J., Zhou, J., Yuan, B., Zhang, Y., Wei, J., Wang, W.: Experimental study of subcooled boiling pool heat transfer and its “hook back” phenomenon on micro/nanostructured surfaces. Int. Commun. Heat. Mass. Transf. **100**, 73–82 (2019)

Liu, B., Yang, X., Jie, Z., Wei, J., Li, Q.: Enhanced pool boiling on micro-nano composited surfaces with nanostructures on micro-pin-fins. Int. J. Heat. Mass. Transf. **190** (2022b)

Liu, B., Yu, L., Zhang, Y., Marco, P.D., Wei, J.: Enhanced Nucleate Pool Boiling by Coupling the Pinning Act and Cluster Bubble Nucleation of Micro-nano Composited Surfaces. Int. J. Heat. Mass. Transf. **157**, 119979 (2020)

Ma, A., Wei, J., Yuan, M., Fang, J.: Enhanced flow boiling heat transfer of FC-72 on micro-pin-finned surfaces. Int. J. Heat Mass Transf. **52**(13–14), 2925–2931 (2009)

Moghadasi, H., Saffari, H.: Experimental study of nucleate pool boiling heat transfer improvement utilizing micro/nanoparticles porous coating on copper surfaces. Int. J. Mech. Sci. **196**, 106270 (2021)

Nguyen, T.B., Liu, D., Kayes, M.I., Wang, B., Rashin, N., Leu, P.W., Tran, T.: Critical heat flux enhancement in pool boiling through increased rewetting on nanopillar array surfaces. Sci. Rep. **8**(1), 4815 (2018)

O’Connor, J.P., You, S.M.: Painting technique to enhance pool boiling heat transfer in saturated FC-72. J. Heat. Transf. **117**(2), 387–393 (1995)

Pastuszko, R.: Pool boiling for extended surfaces with narrow tunnels – Visualization and a simplified model. Exp. Thermal. Fluid Sci. **38**, 149–164 (2012)

Patil, C.M., Kandlikar, S.G.: Pool boiling enhancement through microporous coatings selectively electrodeposited on fin tops of open microchannels. Int. J. Heat. Mass. Transf. **79**, 816–828 (2014)

Rainey, K.N., You, S.M., Lee, S.: Effect of pressure, subcooling, and dissolved gas on pool boiling heat transfer from microporous, square pin-finned surfaces in FC-72. Int. J. Heat. Mass. Transf. **46**(1), 23–35 (2003)

Ray, M., Deb, S., Bhaumik, S.: Pool boiling heat transfer of refrigerant R-134a on TiO2 nano wire arrays surface. Appl. Therm. Eng. **107**, 1294–1303 (2016)

Song, K., Jun, S., You, S.M., Kim, H.Y., Kim, M.H., Revankar, S.T.: Flow boiling heat transfer from downward-facing thick heater block in an inclined channel with plain and microporous coated surfaces. Int. J. Heat. Mass. Transf. **129**, 1010–1022 (2019)

Tang, Y., He, Z., Lu, L., Wang, H., Pan, M.: Burr formation in milling cross-connected microchannels with a thin slotting cutter. Precis. Eng. **35**(1), 108–115 (2011)

Thiagarajan, S.J., Yang, R., King, C., Narumanchi, S.: Bubble dynamics and nucleate pool boiling heat transfer on microporous copper surfaces. Int. J. Heat. Mass. Transf. **89**, 1297–1315 (2015)

Tran, N., Sajjad, U., Lin, R., Wang, C.-C.: Effects of surface inclination and type of surface roughness on the nucleate boiling heat transfer performance of HFE-7200 dielectric fluid. Int. J. Heat. Mass. Transf. **147**, 119015 (2020)

Wang, L., Wang, Y., Cheng, W., Yu, H., Xu, J.: Boiling heat transfer properties of copper surface with different microstructures. Mater. Chem. Phys. **267**, 124589 (2021)

Wei, J.J., Honda, H.: Effects of fin geometry on boiling heat transfer from silicon chips with micro-pin-fins immersed in FC-72. Int. J. Heat. Mass. Transf. **46**(21), 4059–4070 (2003)

Wei, J., Zhao, J., Yuan, M., Xue, Y.: Boiling Heat Transfer Enhancement by Using Micro-pin-finned Surface for Electronics Cooling. Microgravity. Sci. Technol. **21**(S1), 159–173 (2009)

Xu, J., Wang, Y., Yang, R., Liu, W., Wu, H., Ding, Y., Li, Y.: A review of boiling heat transfer characteristics in binary mixtures. Int. J. Heat. Mass. Transf. **164**, 120570 (2021)

Yu, T., Cui, C., Qi, B., Wei, J., Yuan, J., Qaisrani, M.A.: Boiling heat transfer and bubble distribution on inhomogeneous wetting surface patterned with Sierpinski carpet. Appl. Therm. Eng. **180**, 115818 (2020)

Yuan, B., Zhang, Y., Zhou, J., Liu, L., Wei, J.: Critical heat flux prediction model for flow boiling on micro-pin-finned surfaces. Int. J. Heat. Mass. Transf. **154** (2020)

Yuan, M., Wei, J., Xue, Y., Fang, J.: Subcooled flow boiling heat transfer of FC-72 from silicon chips fabricated with micro-pin-fins. Int. J. Therm. Sci. **48**(7), 1416–1422 (2009)

Zhang, Y., Liu, B., Wei, J., Sundén, B., Wu, Z.: Heat transfer correlations for jet impingement boiling over micro-pin-finned surface. Int. J. Heat. Mass. Transf. **126**, 401–413 (2018a)

Zhang, Y., Zhou, J., Zhou, W., Qi, B., Wei, J.: CHF correlation of boiling in FC-72 with micro-pin-fins for electronics cooling. Appl. Therm. Eng. **138**, 494–500 (2018b)

Zhao, J.F., Wan, S.X., Liu, G., Yan, N., Hu, W.R.: Subcooled pool boiling on thin wire in microgravity. Acta. Astronaut. **64**(2–3), 188–194 (2009)

Zhou, J., Liu, B., Qi, B., Wei, J., Mao, H.: Experimental investigations of bubble behaviors and heat transfer performance on micro/nanostructure surfaces. Int. J. Therm. Sci. **135**, 133–147 (2019)

Zhou, J., Qi, B., Zhang, Y., Wei, J., Yang, Y., Cao, Q.: Experimental and theoretical study of bubble coalescence and departure behaviors during nucleate pool boiling on uniform smooth and micro-pin-finned surfaces under different subcoolings and heat fluxes. Exp. Thermal. Fluid. Sci. **112**, 109996 (2020)

Zhou, J., Xu, P., Qi, B., Zhang, Y., Wei, J.: Effects of micro-pin-fins on the bubble growth and movement of nucleate pool boiling on vertical surfaces. Int. J. Therm. Sci. **171**, 107186 (2022)

Publisher's Note Springer Nature remains neutral with regard to jurisdictional claims in published maps and institutional affiliations.